Structural characterization and physical ageing of mucilage from chia for food processing applications

Giovanni Ferraro [a], Emiliano Fratini [a,**], Pasquale Sacco [b], Fioretta Asaro [c], Francesca Cuomo [d], Ivan Donati [b], Francesco Lopez [d,*]

[a] Department of Chemistry "Ugo Schiff" & Center for Colloid and Surface Science (CSGI), University of Florence, Via della Lastruccia 3, 50019, Sesto Fiorentino , Florence, Italy
[b] Department of Life Sciences, University of Trieste, Via Licio Giorgieri 5, I-34127, Trieste, Italy
[c] Department of Chemical and Pharmaceutical Sciences, University of Trieste, Via Licio Giorgieri 1, I-34127, Trieste, Italy
[d] Department of Agricultural, Environmental and Food Sciences (DiAAA), Center for Colloid and Surface Science (CSGI), University of Molise, Via De Sanctis, I-86100, Campobasso, Italy

ARTICLE INFO

Keywords:
Chia seeds
Mucilage
Hydrogels
Microstructure
Rheology
SAXS

ABSTRACT

Chia seed mucilage represents an emerging resource in food industry due to its particular tetrasaccharide (repeating unit) composition. In this investigation, we report on the effect of biomacromolecule concentration and ageing on the structural integrity of chia mucilage-based hydrogel networks. Hydrogels were produced with different polymer concentration and analyzed as prepared and after 10 days of ageing. Structural studies were undertaken through scanning electron microscopy, rheology and small angle X-ray scattering (SAXS). Rheological characterization revealed that ageing acts as destabilizing factor for hydrogel architecture. Indeed, hydrogel strength as well as viscosity were found to decrease upon ageing. This behavior related with a structural change was validated by microscopy. Strikingly, the formation of less entangled and packed meshwork was evidenced. SAXS elucidated that the mesh size of the hydrogel network increased with ageing. Overall, the ageing information provided in this study has to be taken into account when using chia mucilage as a food ingredient or in other application fields.

1. Introduction

Chia mucilage (CM) (*Salvia hispanica* L.*)* is an emerging and attractive constituent in the production of innovative materials for a wide range of advanced applications (Brütsch, Stringer, Kuster, Windhab, & Fischer, 2019). *Salvia hispanica* is an annual herbaceous plant species in the *Lamiaceae* family (Whistler, 1982). The nutritional values of chia seeds have been appreciated and their health benefits have also been documented (Ding et al., 2018; Orona-Tamayo, Valverde, & Paredes-López, 2017; Scheer, 2011; Valdivia-López & Tecante, 2015). The mucilage extracted from chia seeds is a polysaccharide-rich exudate that is attracting increasing interest, especially in food industry (Campos, Ruivo, Silva Scapim, Madrona, & Bergamasco, 2016; Dick et al., 2015). The mucilage released from the seed coat during hydration can be easily extracted and hydrated to achieve water retention, which accounts for its great potential as a functional ingredient for use as a thickening agent (Muñoz Hernández, 2012; Salgado-Cruz et al., 2013). The strong water binding capacity of the hydroxyl groups in the polysaccharide core allows the mucilage to hydrate and thus store enormous water reserves, which can give plants the ability to withstand physiological drought (Clarke, Anderson, & Stone, 1979).

The use of hydrocolloids in the food industry, which includes natural polymers, offers a versatile degree of flexibility for many applications (Cofelice, Lopez, & Cuomo, 2019; Cuomo, Iacovino, Messia, Sacco, & Lopez, 2020; Sacco et al., 2017; Saha & Bhattacharya, 2010). The increasing attention to mucilage has been confirmed by several studies on the structure and composition of mucilages (Capitani et al., 2015; Coorey, Tjoe, & Jayasena, 2014; Timilsena, Wang, Adhikari, & Adhikari, 2016). The ability of these natural materials to form gels/mucilages has important ecological functions such as stability during flooding and survival under harsh environmental conditions (Salgado-Cruz et al., 2013). CM is a typical example of a hydrophilic polymer that forms

* Corresponding author.
** Corresponding author.
E-mail addresses: emiliano.fratini@unifi.it (E. Fratini), lopez@unimol.it (F. Lopez).

Accepted 21 February 2022

suspensions in water with the properties of colloids (hydrocolloids). Despite significant progress in understanding the basic structure-property relationship of such molecules that make up the networks, much remains to be elucidated about how the macromolecular building blocks affect the properties of the sample at the macroscopic level. Clearly, having information on the structure and physical properties of a polymer network as different parameters such as polymer concentration, pH, time and additives vary could be useful for managing this type of material in various industrial applications (Paderes et al., 2020; Santan et al., 2018). When dissolved in water, chia seed mucilage forms a gel-like network that interacts with the seed to form supramolecular complexes (Lin, Daniel, & Whistler, 1994). Samateh et al. (Samateh et al., 2018) have shown that some seeds, such as those of chia (*Salvia hispanica*) and basil (*Ocimum basilicum*), can form hydrogel-like structures when soaked in water without external crosslinkers. This hydrogel-like matrix consists of an extensive network of nanoscale fibers that extends from the surface of the seeds into the aqueous bulk.

It has already been reported that CM displays a high water absorption capacity, which is due to the abundant free hydroxyl groups that can combine with water molecules to form a physical gel (Coorey et al., 2014; Segura-Campos, Ciau-Solís, Rosado-Rubio, Chel-Guerrero, & Betancur-Ancona, 2014). The different water affinity found in several papers was attributed to the different protein and fiber contents of the mucilage species present (Orifici, Capitani, Tomás, & Nolasco, 2018). An important step in studying the structure-property relationship of polymer networks is to reduce network defects, such as inhomogeneity associated with irregular cross-linked junctions and the presence of loops (loose chains). These inhomogeneous components usually form in an unpredictable manner and can affect the resulting physical properties of the network (Saffer et al., 2014).

Ageing is a process that occurs in many polymers when their properties change over time. Once formed, the gel structure is not necessarily static and could continue to evolve due to the instability of the low-energy interactions that bind the gel network. The ageing process of hydrogels is one of the parameters that must be carefully evaluated when manufacturing a product to be used in different applications. In fact, it has been observed that viscosity decreases after storage (Ahmad, Ahmad, Manzoor, Purwar, & Ikram, 2019; Shewan & Stokes, 2013).

Recently, we highlighted that the degradation of CM can be slowed down by the presence of a small amount of lemongrass essential oil, which has antioxidant activity (Cuomo, Iacovino, Cinelli, et al., 2020; Cuomo, Iacovino, Messia, et al., 2020).

Considering the interest in chia mucilage for various applications, it seems to be of key importance to provide experimental evidence for the change in the microstructure of the biomacromolecule over time and to link the structural changes to the amount of water adsorption observed at the macroscopic level. In this work, a structural study performed by FTIR spectroscopy, small angle X-ray scattering (SAXS), rheology and microscopy on CM hydrogels is reported. The role of biopolymer concentration and preservation over time was evaluated. Our main focus was to understand the initial structure of CM and the changes that occur after several days of ageing. Therefore, in this study a multi-technical approach was used to make important evaluations on the structure of chia along with the induced ageing effects.

2. Materials and methods

Materials. Chia seeds (*Salba grain organic*) were obtained from I.P.A. s. r.l. Industria Prodotti Agroalimentari (Viterbo, Italy). Milli-Q water (18.2 MΩ) was employed for all the experiments.

Mucilage extraction from chia seeds. Chia seeds were weighted and placed in a vessel with ultrapure water in a 1:20 (w/w) ratio for 12 h to extract CM. The CM was recovered through vacuum filtration with a Buchner funnel, frozen at −40 °C and then freeze-dried under vacuum in a Genesis 25 ES (VirTis, NY, USA) for 48 h (maximum shelves' temperature 20 °C). After freeze-drying, CM had the aspect of a dried foam and was stored at room temperature.

Samples preparation. The freeze-dried CM was dispersed in warm milli-Q water (50 °C) under stirring until complete disappearance of macroscopic aggregates. CM suspensions were stored in glass containers with Teflon-lined caps analyzed immediately (fresh) and after 10 days (aged). After the preparation the samples were stored at 25 °C at ambient condition.

Infrared spectroscopy (IR). The FTIR spectra were acquired in transmission mode from KBr pellets, over the 4000-400 cm^{-1} wavenumber interval with 4 cm^{-1} instrumental resolution, by a Perkin Elmer Spectrum2000R FTIR spectrometer.

Rheology. Rheological measurements were carried out using a rheometer (Haake MARS III-Thermo Scientific, Karlsruhe, Germany) equipped with a 20 mm cone (1° angle) plate geometry probe (CP20). The instrument was equipped with a Peltier element combined with a Phoenix II digital system (Thermo Scientific, Karlsruhe, Germany) for the temperature control. Samples (40 μL) were left equilibrating for 5 min before measurements (Cofelice et al., 2019). Rotational tests were carried out in controlled rate varying the shear rate from 1 to 200 s^{-1}. Oscillation strain sweep measurements were carried out for determining the linear viscoelastic range (LVE) at a fixed frequency of 1 Hz. Frequency sweep tests were performed using a fixed strain ($\gamma = 0.003$) within the LVE and in a range of frequency from 0.1 to 10 rad s^{-1}. The storage (G′) and loss moduli (G″) were determined as a function of frequency (Cuomo, Cofelice, & Lopez, 2019; Mezger, 2006).

Scanning Electron Microscopy (SEM). SEM experiments were performed using a high-resolution scanning electron microscope (ΣIGMA, Carl Zeiss) based on the GEMINI column, which features a high brightness Schottky field emission source, beam booster, and in-lens secondary electron detector. The micrographs were acquired on uncoated samples with an acceleration potential of 1 kV and a working distance of about 3 mm. All the samples were analyzed after freeze-drying treatment. All the micrographs were analyzed with an image processing software (ImageJ, v.1.49. p) (Schneider, Rasband, & Eliceiri, 2012) in order to evaluate the fibers' diameter distribution (more than 100 fibers for each sample were measured) according to a procedure already reported in the literature (Hotaling, Bharti, Kriel, & Simon, 2015).

Optical Microscopy. A Nikon Eclipse Ti–S Inverted Microscope was used to obtain optical micrographs of the liquid dispersions. All measurements were performed using an objective with a 10× magnification.

Small-angle X-ray scattering. Small-angle X-ray scattering (SAXS) measurements were performed using a HECUS S3-Micro (Kratky camera) equipped with two position-sensitive detectors (PSD-50M) containing 1024 channels of 54-μm width. Cu Kα radiation, $\lambda = 1.542$ Å, was provided by a GeniX (Xenocs, Grenoble) X-ray generator (sealed-tube type, microfocus), operating at power of 50 W customized whit a high-brillance microbeam delivery system with point-focus multilayer optics (FOX3D; Xenocs, Grenoble, France) able to remove Cu K_β radiation. The sample-to-detector distance was 281 mm and the volume was kept under vacuum during the measurements to minimize scattering from the air. The Kratky camera was calibrated using silver behenate, which is known to have a well-defined lamellar structure (d = 58.34 Å) (Blanton et al., 1995). Scattering curves were acquired in a hot-glue sealed borosilicate glass capillary tube at 25 °C in the q-range 0.014–0.55 $Å^{-1}$, where $q = 2\pi/\lambda \sin\theta$ is the scattering vector at a scattering angle of 2θ. The temperature was controlled by a Peltier element, with an accuracy of ±0.1 °C. The contribution of the capillary tube/water was subtracted out from all curves considering the relative transmission factor. Desmearing of the SAXS curves was not necessary because of the sophisticated point microfocusing system.

3. Results and discussion

Chia physical gels were obtained by dissolving freeze-dried CM in

water. Freshly prepared CM hydrogels were compared with analogous samples stored at room temperature for 10 days. A visual inspection of the freshly prepared hydrogels revealed a significant turbidity enhancement, as well as important viscosity increase, as the weight fraction of mucilage increased (Cuomo, Iacovino, Cinelli, et al., 2020). The freeze-dried mucilage of chia seeds used for this study contains about 75% of fibers and 10% of proteins. For yield of extraction and proximate analyses see elsewhere (Cuomo, Iacovino, Messia, et al., 2020).

3.1. Composition

IR spectroscopy was used to identify the functional groups involved in water binding and to compare freshly prepared and aged hydrogels. The IR spectra of the freeze-dried chia mucilages are reported in Fig. 1a. Fig. S1 shows the second derivatives, which provides better resolution of the signals.

As shown, the typical bands for polysaccharides dominate, which is consistent with the composition of the mucilages (Lin et al., 1994) and previous literature on chia mucilage (Ellerbrock, Ahmed, & Gerke, 2019; García-Salcedo, Torres-Vargas, del Real, Contreras-Jiménez, & Rodriguez-Garcia, 2018; Goh et al., 2016). The broad band around 3400 cm^{-1} corresponds to the O–H stretching of hydrogen-bonded O–H groups, including that of adsorbed/hydration water. The asymmetric and symmetric C–H stretching appears at 2923 cm^{-1} and 2854 cm^{-1}, respectively. At 1630 cm^{-1}, the water deformation band merges with the signal of the asymmetric stretching of the COO^- group of uronic acids at 1596 cm^{-1} in the 2nd derivative spectrum (Fig. S1), while the COO^- symmetric stretching is at about 1420 cm^{-1} and overlaps with the bending of the CH_2 group (Kačuráková & Wilson, 2001).

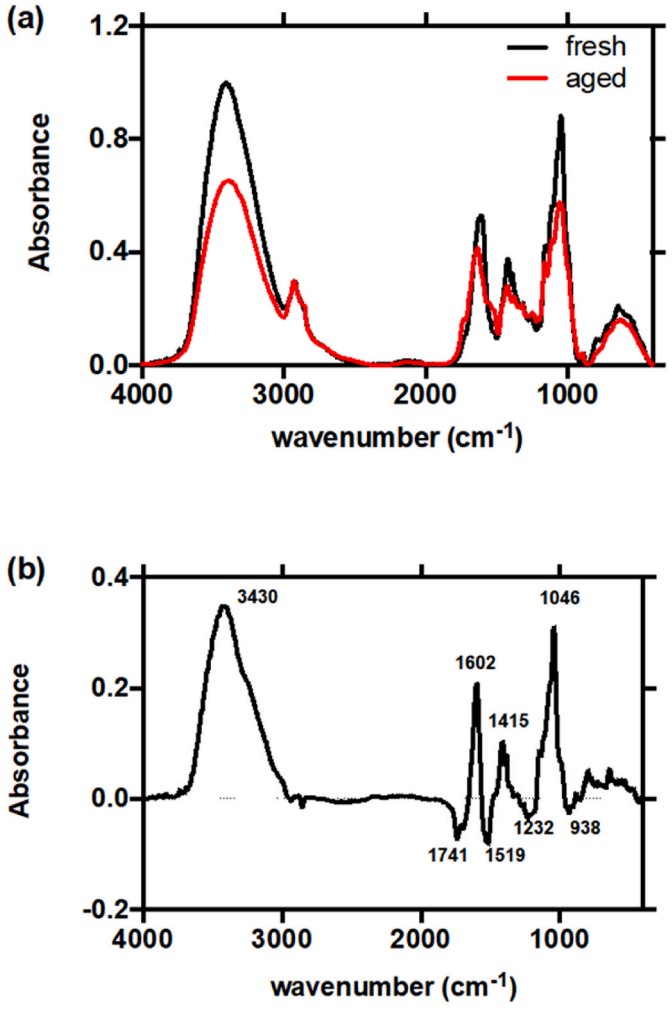

Fig. 1. (a) IR spectra of CM hydrogels freshly prepared (black line) and after ageing for 10 days (red line). **(b)** Difference spectrum between CM fresh prepared and after ageing. (For interpretation of the references to colour in this figure legend, the reader is referred to the Web version of this article.)

The strongest signal is the envelope in the 1200–900 cm^{-1} range of COH bending signals, stretching vibrations of C–O and C–C bonds, and asymmetric C–O–C stretching of both sugar rings and glycosidic links (Kačuráková & Wilson, 2001). The characteristic band of the beta-anomer appears at 897 cm^{-1}, in agreement with the configuration reported for xylose in CM polysaccharides (Lin et al., 1994).

Comparison of the IR spectra for CM before and after aging, normalized to the intensity of the CH stretching bands (Fig. 1b), shows a decrease in the intensity of the signals from carboxylate groups and, in particular, the band in the 1200-900 cm^{-1} range, possibly reflecting in a decrease number of glycosidic linkages. On the other hand, the peaks at about 1550 cm^{-1} and in the 1400-1200 cm^{-1} range appear more distinct. These signals may be attributed to the non-polysaccharide portion of the material, particularly to slight protein contamination, as these positions correspond to the amide II and amide III bands of the protein backbone, respectively (Timilsena et al., 2016). Similar IR spectral variations were reported for the outer region of a freeze-dried chia mucilage droplet and attributed to oxidation processes. A varied composition of the organic matter in the outer region of the droplet likely results in increased C═O/C–O–C and reduced C–H/C═O ratios toward the droplet rim (Ellerbrock et al., 2019).

3.2. Mechanical properties and morphology

The characteristic polysaccharide composition of CM is responsible for hydrogel formation and its rheological behaviour (Read & Gregory, 1997). Fig. 2a shows the apparent viscosity of CM hydrogel as a function of the shear rate. As can be seen, viscosity either for fresh or aged CM decreased with the shear rate, showing shear thinning behavior. Overall viscosity of aged CM was lower than fresh CM, indicating that the characteristics of the hydrogel were modified by ageing. Moreover, oscillations at high shear rate detected only in the aged sample indicated slippage phenomena due to the very unstable structure. The viscoelastic performance of polymers depends on the degree and functionality of interactions. The plot of the elastic (G′) and viscous (G″) moduli versus the applied deformation (γ) at time 0 and after 10 days for a sample at 1% CM concentration is reported in Fig. 2b. As shown, when the storage time increases from 0 to 10 days, the hydrogel elastic response (G′) decreases and the LVE was reduced (upper strain limit of LVE was around 0.052 for fresh CM and around 0.013 for aged CM), indicating the occurrence of phenomena that destabilize the hydrogel network. Frequency sweep tests (Fig. 2c) carried out on fresh samples and on aged counterparts show that after 10 days the gel-like behavior of the CM hydrogels is preserved since the storage modulus (G′) is still higher than the loss modulus (G″) despite the decrease of their absolute values.

Rheological results prompted us to further characterize the morphology of CM hydrogels as prepared and after 10 days ageing by means of scanning electron microscopy. The micrographs of freeze-dried chia seed mucilage before and after dispersion in water (1 wt%) immediately after sample preparation are reported in Fig. 3.

The micrographs of lyophilized CM in Fig. 3a and c show the presence of aggregated laminar foils due to the extraction procedure as previously described (Tavares, Junqueira, de Oliveira Guimarães, & de Resende, 2018). The CM 1 wt% water dispersion (Fig. 3b and d) shows two different populations of fibers with a dimension of around 20 and 500 nm, respectively (see distribution in Fig. S2 and Table S1, SI file). This morphology comes from the disentanglement of the polysaccharide chains in water, and is responsible for the peculiar rheological properties of these systems. Salgado-Cruz and co-workers reported a fiber diameter ranging from 15 to 45 nm (Salgado-Cruz et al., 2013). Other authors

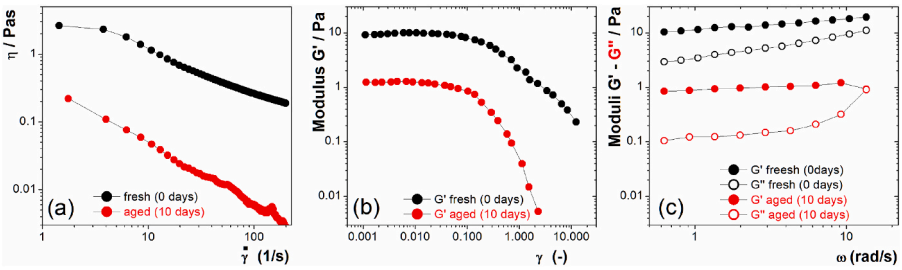

Fig. 2. Rheological response of CM hydrogels at a concentration of 1 wt% as prepared (black symbols) after 10 days of ageing (red symbols). **(a)** Viscosity curves through rotational tests, **(b)** strain sweep and **(c)** frequency sweep of CM hydrogels. (For interpretation of the references to colour in this figure legend, the reader is referred to the Web version of this article.)

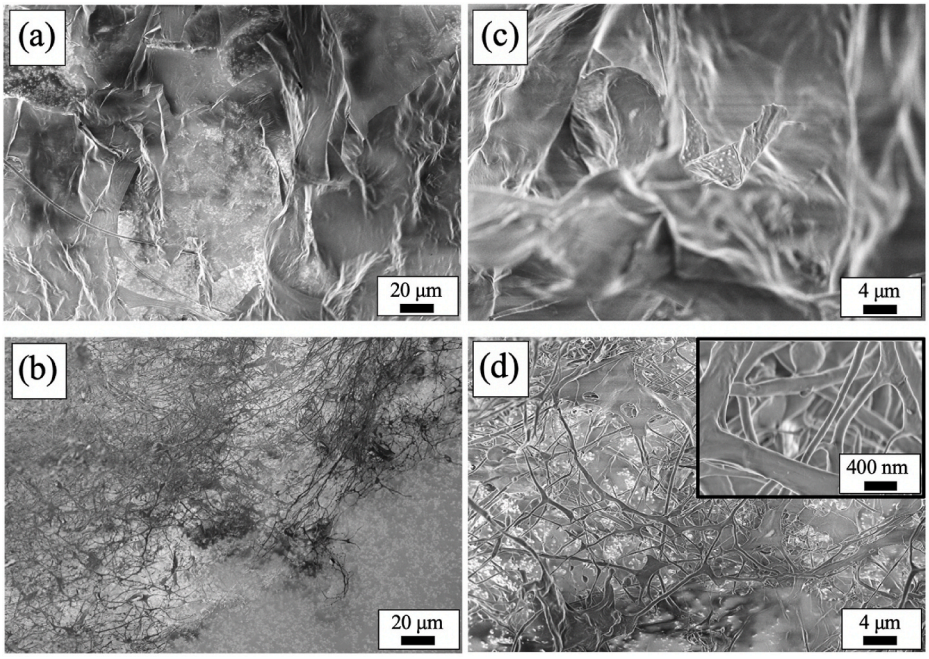

Fig. 3. SEM micrographs at different magnifications (1 kX and 5 kX) showing the freeze-dried CM after the extraction procedure **(a, c)** and after the preparation of the 1 wt% dispersion **(b, d)**.

found cellulose fibers of 3.5 nm width and 10 nm length (Nakagaito & Yano, 2004). The discrepancy detected for fibers dimension could be ascribed to the different approach used for the dispersion of CM in water or the different sample preparation before microscopy experiments.

The SEM micrograph for aged 1 wt% CM dispersion shows an evident modification of the fibers network and morphology (Fig. 4b). In particular, a more disentangled network and less defined fibers' structure are revealed. Similar results come from optical micrographs (Fig. 4c and d), showing a different morphology of the 10 days aged sample if compared with the as prepared analogous. In particular, the aged sample shows less defined fibers and a higher amount of inhomogeneity degree.

The morphological changes observed upon ageing can explain the different mechanical behavior of CM water dispersions as passing time. The outcomes of rheology and inspection are in agreement with previous works that proved mucilage breaks down toward a water-like substance over an ageing of two weeks (Van Veelen, Tourell, Koebernick, Pileio, & Roose, 2018) and this change from a higher to a lower viscosity system was ascribed to the degradation of mucilage to a more aqueous gel-like network (Naveed et al., 2017).

3.3. Microstructure

SAXS analysis was carried out on chia physical hydrogels prepared using three polymer concentrations (0.2, 1 and 2 wt%) at time 0 and after 10 days ageing. Fig. 5 reports the scattering curves for all the investigated systems together with the best fits obtained using the correlation length model (Hammouda, Ho, & Kline, 2004), while Table 1 lists the parameters obtained from the fitting. In this model, which has been used with some slight modifications to describe the structure of entangled charged polymer chains (Carretti, Matarrese, Fratini, Baglioni, & Dei, 2014), the scattering intensity, I(q), is calculated as:

$$I(q) = \frac{C}{1 + (q\xi)^m} + bkg \quad (1)$$

where m is the Lorentzian exponent, C is a scale factor, ξ is the correlation length for the polymer chains or mesh size and bkg is an instrumental background. The Lorentzian exponent characterizes the polymer–solvent interactions (Saffer et al., 2014) and is inversely proportional to the excluded volume parameter, $\nu = 1/m$. In particular, $m = 5/3$ refers to polymers in a good solvent (monomer-solvent interaction is more favourable than monomer–monomer interaction), for $m = 2$ the monomer–solvent and monomer–monomer interactions are equal in strength (theta solvent condition) and $m > 2$ corresponds to a state where the polymer is collapsed (i.e., bad solvent case).

It is worth noting that the correlation length model gives valuable results for polymer solutions in the semi-dilute regimes (Yukioka, Higo,

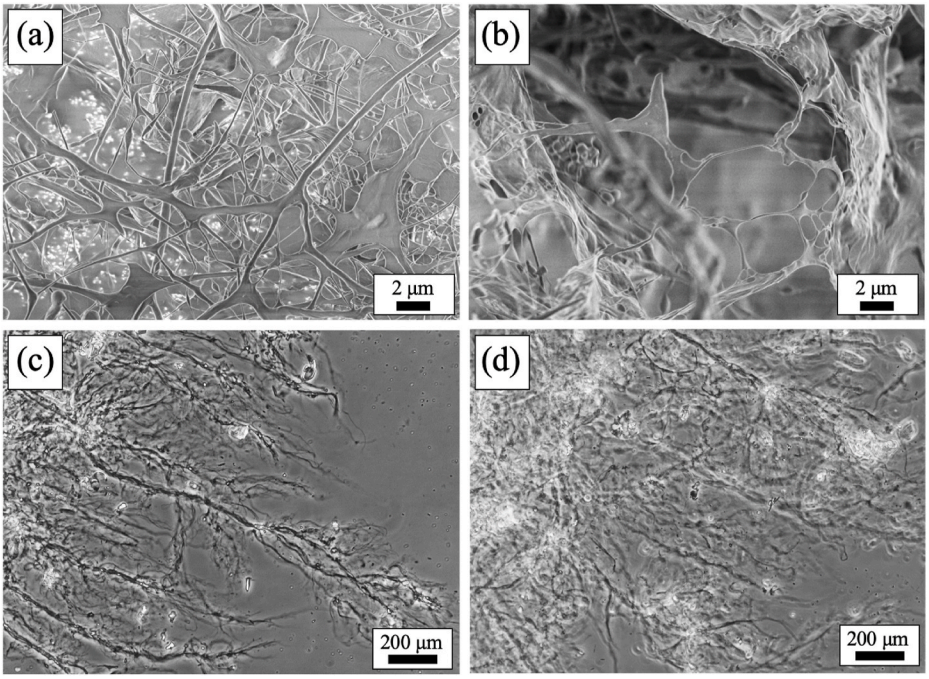

Fig. 4. SEM micrographs (magnification: 10 kX) of CM fibers in water (1 wt%) **(a)** as prepared and **(b)** after 10 days of ageing. **(c, d)** optical micrographs (magnification: 10×) for fresh and aged CM dispersions.

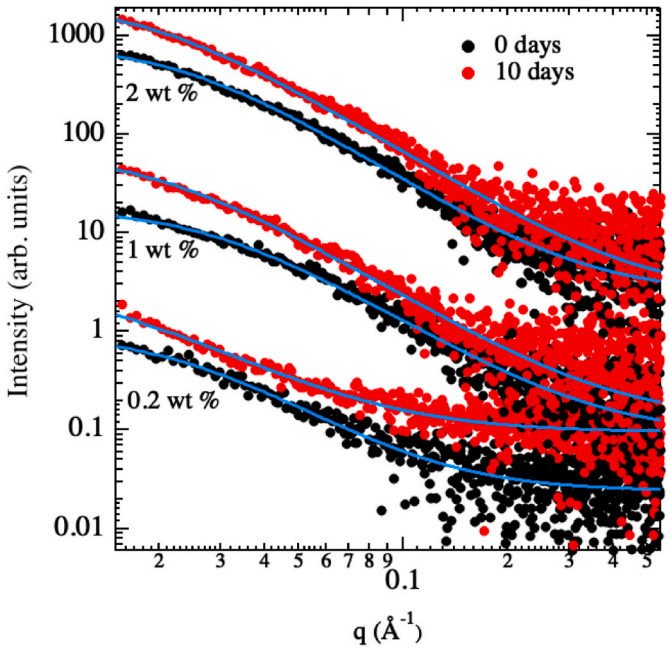

Fig. 5. Scattering curves in arbitrary units for fresh (black markers) and aged (red markers) CM water dispersions (0.2 wt%, 1 wt% and 2 wt%) along with the best fits obtained using the correlation length model (continuous lines). (For interpretation of the references to colour in this figure legend, the reader is referred to the Web version of this article.)

Noda, & Nagasawa, 1986). In our systems, the critical concentration of chain entanglement C^*, which ideally sets dilute from semi-dilute regimes, was calculated by taking the reverse of the intrinsic viscosity, $1/([\eta])$ (Cuomo, Iacovino, Messia, et al., 2020), and resulted 0.25 g/L (i.e. 0.025 wt%). This value is in good agreement with previous findings (Timilsena et al., 2016), and we can claim that the investigated CM dispersions are in the semi-diluted regime (Hammouda et al., 2004; Paladini et al., 2019; Saffer et al., 2014).

Table 1
Parameters obtained from the fit of the scattering curves using the correlation length model. Values in parentheses are standard deviations on the last significant figure.

	0 days (fresh)			10 days (aged)		
	0.2%	1%	2%	0.2%	1%	2%
scale	0.005(3)	0.51(1)	2.26(6)	0.25(3)	0.43(1)	0.779(9)
bkg	0.053(2)	0.026(3)	0.054(4)	0.101(2)	0.01(2)	0.01(2)
C	475.1(9)	12.26(6)	8.75(5)	14.01(9)	11.5(5.3)	12.7(6)
ξ (Å)	43(2)	35(1)	42(1)	78(2)	50(2)	52(1)
m	2.18(7)	2.11(4)	2.23(3)	1.88(4)	2.10(2)	2.14(2)
χ^2	2.4	1.7	1.5	1.4	1.6	1.6

The results reveal that the correlation length (ξ) increases with the ageing of the samples. The correlation length corresponds to a mesh (or "blob") size characteristic of the polymer concentration/conformation. Indeed, the disassembly of the polymer network observed by microscopy leads to a less entangled structure with the formation of less packed regions. The exponent m is roughly 2 for all samples, independently from the ageing time and/or concentration of CM in water. m depends on the balance between the polymer/polymer and polymer/solvent interactions (Hammouda et al., 2004). The m value found for our CM samples indicates that the polymer-solvent and polymer-polymer interactions are comparable in strength corresponding to a theta solvent situation.

It is also possible to obtain a good fit of the experimental SAXS profiles using the flexible cylinders model (Pedersen & Schurtenberger, 1996). The good agreement between fit and experimental points is reported in Fig. S3. This approach has been already reported in the literature for analogous systems, as for example dispersions of cellulose nano-fibrils in water with different concentrations (Paladini et al., 2019; Schmitt et al., 2018). In this work, the authors describe the Kuhn length as directly associated to the mesh size of the gel network. In our case, the values obtained for the diameter of the fibers range from around 2 to 3 nm while the Kuhn length is between 4 and 8 nm.

The importance of the rheological and size characterization on the

gelatin gels microstructure evolution was previously reported by Tosh et al. (Tosh, Marangoni, Hallett, & Britt, 2003). The authors demonstrated that gelatin gels could be manipulated by adjusting the setting temperature. The SAXS data, together with the mechanical properties that highlighted a decrease of the resistance of the hydrogels after 10 days of storage, suggested by means of the complex viscosity analysis the different morphology of the samples observed also by the detailed microscopy study that lead us to confirm that CM hydrogels is affected by ageing modifications most probably connected with oxidation processes accompanied by chain scission of the pristine polysaccharides (White, 2006), as confirmed by IR results reported in this study. This is in accordance with our recent studies where we proposed a fluorimetric method to prove oxidative/autooxidative phenomena based on thermal activation of heat-labile azo compounds (Cuomo, Iacovino, Cinelli, et al., 2020; Cuomo, Iacovino, Messia, et al., 2020). On the same line Hernández-Morales et al. (Hernández-Morales et al., 2019) exploited the oxidative susceptibility of CM for the green synthesis of Ag nanoparticles starting from silver nitrate. In particular, the authors highlighted the synergistic occurrence of the oxidation of polysaccharides and the reduction of Ag.

Although bacterial contamination cannot be a priori excluded for longer period of time, in our experimental conditions also in view of previous experimental evidences, CM degradation has to be considered the real key role that induces the observed modifications.

At the same time, it cannot be excluded that a number of age related phenomena could operate simultaneously and interactively. Considering that chia mucilage seems to offer high potentiality in food technologies like gelling, thickening and coating, the matrix evolution induced by time should be not necessarily considered a harm (Saha & Bhattacharya, 2010). Finally, one also should bear in mind that most of the biotechnological fields in which chia is implied require the use of freshly prepared dispersions of the polysaccharide. However, from this investigation, we outlined the importance of ageing effects occurring after some days of conservation on the structural modification.

4. Conclusions

In this investigation, we studied the effect of polymer concentration and ageing on the mechanical properties of chia mucilage hydrogels. Rheological characterization highlighted that ageing destabilizes the hydrogel network. Indeed, the hydrogel elastic modules (G') decreases and the linear viscoelastic range is reduced, as well as the viscosity shows a decrease of the resistance to flow of the viscoelastic fluid. This behavior can be correlated with a structural change observed by microscopy, in particular the formation of less entangled and packed structures. This was further confirmed by SAXS analysis, which helped us to find that the correlation length (*i.e.*, mesh size) of the hydrogel network increases with the ageing of the samples. In view of the wide range of chia mucilage potential applications in food industry, considering the variability of the mucilage composition depending on its origin and on the production procedure, the crucial role of ageing could represent a significant information for food processing involving chia polymer.

Author statement

Conceptualization: Francesco Lopez, Emiliano Fratini.

Methodology: Emiliano Fratini, Francesca Cuomo, Francesco Lopez.

Software: Giovanni Ferraro, Francesca Cuomo, Pasquale Sacco.

Validation: Emiliano Fratini, Ivan Donati, Francesco Lopez.

Investigation Conducting a research and investigation process, specifically performing the experiments, or data/evidence collection: Giovanni Ferraro, Fioretta Asaro, Francesca Cuomo and Pasquale Sacco.

Data Curation Management activities to annotate (produce metadata), scrub data and maintain research data (including software code, where it is necessary for interpreting the data itself) for initial use and later reuse: Emiliano Fratini; Francesco Lopez; Ivan Donati.

Writing - Original Draft Preparation, creation and/or presentation of the published work, specifically writing the initial draft (including substantive translation): Emiliano Fratini; Francesco Lopez.

Writing - Review & Editing Preparation, creation and/or presentation of the published work by those from the original research group, specifically critical review, commentary or revision – including pre-or postpublication stages: Emiliano Fratini; Francesco Lopez.

Supervision Oversight and leadership responsibility for the research activity planning and execution, including mentorship external to the core team: Emiliano Fratini; Francesco Lopez.

Declaration of competing interest

The authors declare that there is no conflict of interest regarding the publication of this article. All co-authors agreed with the contents of the manuscript. I certify that the submission is original work and is not under review at any other publication.

Acknowledgments

This paper was supported by MIPAAF 2015–2020, project *Profood IV*, CUP: B64E20000180005, **Codice ARS01_00755** and partially supported by CSGI (Centre for Colloid and Surface Science). We acknowledge partial financial support from MIUR "Progetto Dipartimenti di Eccellenza 2018–2022" allocated to Department of Chemistry "Ugo Schiff".

References

Ahmad, S., Ahmad, M., Manzoor, K., Purwar, R., & Ikram, S. (2019). A review on latest innovations in natural gums based hydrogels: Preparations & applications. *International Journal of Biological Macromolecules, 136*, 870–890.

Blanton, T. N., Huang, T. C., Toraya, H., Hubbard, C. R., Robie, S. B., Louër, D., et al. (1995). JCPDS–International Centre for Diffraction Data round robin study of silver behenate. A possible low-angle X-ray diffraction calibration standard. *Powder Diffraction, 10*, 91–95.

Brütsch, L., Stringer, F. J., Kuster, S., Windhab, E. J., & Fischer, P. (2019). Chia seed mucilage–a vegan thickener: Isolation, tailoring viscoelasticity and rehydration. *Food & Function, 10*(8), 4854–4860.

Campos, B. E., Ruivo, T. D., Silva Scapim, M. R., Madrona, G. S., & Bergamasco, R. d C. (2016). Optimization of the mucilage extraction process from chia seeds and application in ice cream as a stabilizer and emulsifier. *LWT-Food Science and Technology, 65*, 874–883.

Capitani, M., Corzo-Rios, L., Chel-Guerrero, L., Betancur-Ancona, D., Nolasco, S., & Tomás, M. (2015). Rheological properties of aqueous dispersions of chia (Salvia hispanica L.) mucilage. *Journal of Food Engineering, 149*, 70–77.

Carretti, E., Matarrese, C., Fratini, E., Baglioni, P., & Dei, L. (2014). Physicochemical characterization of partially hydrolyzed poly(vinyl acetate)–borate aqueous dispersions. *Soft Matter, 10*(25), 4443–4450. https://doi.org/10.1039/C4SM00355A

Clarke, A. E., Anderson, R. L., & Stone, B. A. (1979). Form and function of arabinogalactans and arabinogalactan-proteins. *Phytochemistry, 18*(4), 521–540. https://doi.org/10.1016/S0031-9422(00)84255-7

Cofelice, M., Lopez, F., & Cuomo, F. (2019). Quality control of fresh-cut apples after coating application. *Foods, 8*(6). https://doi.org/10.3390/foods8060189

Coorey, R., Tjoe, A., & Jayasena, V. (2014). Gelling properties of chia seed and flour. *Journal of Food Science, 79*(5), 859–866.

Cuomo, F., Cofelice, M., & Lopez, F. (2019). Rheological characterization of hydrogels from alginate-based nanodispersion. *11*(2).

Cuomo, F., Iacovino, S., Cinelli, G., Messia, M. C., Marconi, E., & Lopez, F. (2020). Effect of additives on chia mucilage suspensions: A rheological approach. *Food Hydrocolloids, 109*. https://doi.org/10.1016/j.foodhyd.2020.106118

Cuomo, F., Iacovino, S., Messia, M. C., Sacco, P., & Lopez, F. (2020). Protective action of lemongrass essential oil on mucilage from chia (Salvia hispanica) seeds. *Food Hydrocolloids, 105*, Article 105860. https://doi.org/10.1016/j.foodhyd.2020.105860

Dick, M., Costa, T. M. H., Gomaa, A., Subirade, M., Rios, A. d O., & Flôres, S. H. (2015). Edible film production from chia seed mucilage: Effect of glycerol concentration on its physicochemical and mechanical properties. *Carbohydrate Polymers, 130*, 198–205. https://doi.org/10.1016/j.carbpol.2015.05.040

Ding, Y., Lin, H.-W., Lin, Y.-L., Yang, D.-J., Yu, Y.-S., Chen, J.-W., et al. (2018). Nutritional composition in the chia seed and its processing properties on restructured ham-like products. *Journal of Food and Drug Analysis, 26*(1), 124–134.

Ellerbrock, R. H., Ahmed, M. A., & Gerke, H. H. (2019). Spectroscopic characterization of mucilage (Chia seed) and polygalacturonic acid. *Journal of Plant Nutrition and Soil Science, 182*(6), 888–895.

García-Salcedo, Á. J., Torres-Vargas, O. L., del Real, A., Contreras-Jiménez, B., & Rodriguez-Garcia, M. E. (2018). Pasting, viscoelastic, and physicochemical properties of chia (Salvia hispanica L.) flour and mucilage. *Food Structure, 16*, 59–66.

Goh, K. K. T., Matia-Merino, L., Chiang, J. H., Quek, R., Soh, S. J. B., & Lentle, R. G. (2016). The physico-chemical properties of chia seed polysaccharide and its microgel dispersion rheology. *Carbohydrate Polymers, 149*, 297–307.

Hammouda, B., Ho, D. L., & Kline, S. (2004). Insight into clustering in poly(ethylene oxide) solutions. *Macromolecules, 37*(18), 6932–6937. https://doi.org/10.1021/ma049623d

Hernández-Morales, L., Espinoza-Gómez, H., Flores-López, L. Z., Sotelo-Barrera, E. L., Núñez-Rivera, A., Cadena-Nava, R. D., et al. (2019). Study of the green synthesis of silver nanoparticles using a natural extract of dark or white Salvia hispanica L. seeds and their antibacterial application. *Applied Surface Science, 489*, 952–961. https://doi.org/10.1016/j.apsusc.2019.06.031

Hotaling, N. A., Bharti, K., Kriel, H., & Simon, C. G., Jr. (2015). DiameterJ: A validated open source nanofiber diameter measurement tool. *Biomaterials, 61*, 327–338.

Kačuráková, M., & Wilson, R. H. (2001). Developments in mid-infrared FT-IR spectroscopy of selected carbohydrates. *Carbohydrate Polymers, 44*(4), 291–303.

Lin, K.-Y., Daniel, J. R., & Whistler, R. L. (1994). Structure of chia seed polysaccharide exudate. *Carbohydrate Polymers, 23*(1), 13–18.

Mezger, T. G. (2006). *The rheology handbook: For users of rotational and oscillatory rheometers*. Vincentz Network GmbH & Co KG.

Muñoz Hernández, L. (2012). *Mucilage from chia seeds (Salvia hispanica): Microestructure, physico-chemical characterization and applications in food industry*.

Nakagaito, A. N., & Yano, H. (2004). The effect of morphological changes from pulp fiber towards nano-scale fibrillated cellulose on the mechanical properties of high-strength plant fiber based composites. *Applied Physics A, 78*(4), 547–552. https://doi.org/10.1007/s00339-003-2453-5

Naveed, M., Brown, L. K., Raffan, A. C., George, T. S., Bengough, A. G., Roose, T., et al. (2017). Plant exudates may stabilize or weaken soil depending on species, origin and time. *European Journal of Soil Science, 68*(6), 806–816.

Orifici, S. C., Capitani, M. I., Tomás, M. C., & Nolasco, S. M. (2018). Optimization of mucilage extraction from chia seeds (*Salvia hispanica* L.) using response surface methodology. https://doi.org/10.1002/jsfa.8974, 98, 12.

Orona-Tamayo, D., Valverde, M. E., & Paredes-López, O. (2017). Chapter 17—chia—the new golden seed for the 21st century: Nutraceutical properties and technological uses. In S. R. Nadathur, J. P. D. Wanasundara, & L. Scanlin (Eds.), *Sustainable protein sources* (pp. 265–281). Academic Press.

Paderes, M. C., James, C., Jamieson, S. A., Mai, A. H., Limon, J. H., Dolatkhani, M., et al. (2020). Tuning the properties of polyether alkyl urea derivatives as rheology modifiers in cosmetic solvents. *ACS Applied Polymer Materials, 2*(7), 2902–2909.

Paladini, G., Venuti, V., Almásy, L., Melone, L., Crupi, V., Majolino, D., et al. (2019). Cross-linked cellulose nano-sponges: A small angle neutron scattering (SANS) study. *Cellulose, 26*(17), 9005–9019. https://doi.org/10.1007/s10570-019-02732-2

Pedersen, J. S., & Schurtenberger, P. (1996). Scattering functions of semiflexible polymers with and without excluded volume effects. *Macromolecules, 29*(23), 7602–7612.

Read, D. B., & Gregory, P. J. (1997). Surface tension and viscosity of axenic maize and lupin root mucilages. *New Phytologist, 137*(4), 623–628.

Sacco, P., Decleva, E., Tentor, F., Menegazzi, R., Borgogna, M., Paoleti, S., et al. (2017). Butyrate-loaded chitosan/hyaluronan nanoparticles: A suitable tool for sustained inhibition of ROS release by activated neutrophils. *Macromolecular Bioscience, 17*(11), 418–426. https://doi.org/10.1002/mabi.201700214

Saffer, E. M., Lackey, M. A., Griffin, D. M., Kishore, S., Tew, G. N., & Bhatia, S. R. (2014). SANS study of highly resilient poly(ethylene glycol) hydrogels. *Soft Matter, 10*(12), 1905–1916. https://doi.org/10.1039/C3SM52395K

Saha, D., & Bhattacharya, S. (2010). Hydrocolloids as thickening and gelling agents in food: A critical review. *Journal of Food Science & Technology, 47*(6), 587–597.

Salgado-Cruz, M. d l P., Calderón-Domínguez, G., Chanona-Pérez, J., Farrera-Rebollo, R. R., Méndez-Méndez, J. V., & Díaz-Ramírez, M. (2013). Chia (Salvia hispanica L.) seed mucilage release characterisation. A microstructural and image analysis study. *Industrial Crops and Products, 51*, 453–462. https://doi.org/10.1016/j.indcrop.2013.09.036

Samateh, M., Pottackal, N., Manafirasi, S., Vidyasagar, A., Maldarelli, C., & John, G. (2018). Unravelling the secret of seed-based gels in water: The nanoscale 3D network formation. *Scientific Reports, 8*(1), 7315. https://doi.org/10.1038/s41598-018-25691-3

Santan, H. D., James, C., Fratini, E., Martínez, I., Valencia, C., Sánchez, M. C., et al. (2018). Structure-property relationships in solvent free adhesives derived from castor oil. *Industrial Crops and Products, 121*, 90–98.

Scheer, J. F. (2011). *The magic of chia: Revival of an ancient wonder food*. North Atlantic Books.

Schmitt, J., Calabrese, V., Da Silva, M. A., Lindhoud, S., Alfredsson, V., Scott, J. L., et al. (2018). TEMPO-oxidised cellulose nanofibrils; probing the mechanisms of gelation via small angle X-ray scattering. *Physical Chemistry Chemical Physics, 20*(23), 16012–16020.

Schneider, C. A., Rasband, W. S., & Eliceiri, K. W. (2012). NIH image to ImageJ: 25 years of image analysis. *Nature Methods, 9*(7), 671–675.

Segura-Campos, M. R., Ciau-Solís, N., Rosado-Rubio, G., Chel-Guerrero, L., & Betancur-Ancona, D. (2014). Chemical and functional properties of chia seed (Salvia hispanica L.) gum. *International Journal of Food Science, 2014*, Article 241053.

Shewan, H. M., & Stokes, J. R. (2013). Review of techniques to manufacture micro-hydrogel particles for the food industry and their applications. *Journal of Food Engineering, 119*(4), 781–792. https://doi.org/10.1016/j.jfoodeng.2013.06.046

Tavares, L. S., Junqueira, L. A., de Oliveira Guimarães, Í. C., & de Resende, J. V. (2018). Cold extraction method of chia seed mucilage (Salvia hispanica L.): Effect on yield and rheological behavior. *Journal of Food Science & Technology, 55*(2), 457–466.

Timilsena, Y. P., Wang, B., Adhikari, R., & Adhikari, B. (2016). Preparation and characterization of chia seed protein isolate–chia seed gum complex coacervates. *Food Hydrocolloids, 52*, 554–563.

Tosh, S. M., Marangoni, A. G., Hallett, F. R., & Britt, I. J. (2003). Aging dynamics in gelatin gel microstructure. *Food Hydrocolloids, 17*(4), 503–513.

Valdivia-López, M.Á., & Tecante, A. (2015). Chapter two—chia (Salvia hispanica): A review of native Mexican seed and its nutritional and functional properties. In J. Henry (Ed.), *Advances in food and nutrition research* (Vol. 75, pp. 53–75). Academic Press.

Van Veelen, A., Tourell, M. C., Koebernick, N., Pileio, G., & Roose, T. (2018). Correlative visualization of root mucilage degradation using X-ray CT and MRI. *Frontiers in Environmental Science, 6*, 32.

Whistler, R. L. (1982). Industrial gums from plants: Guar and chia. *Economic Botany, 36*(2), 195–202.

White, J. R. (2006). Polymer ageing: Physics, chemistry or engineering? Time to reflect. *Comptes Rendus Chimie, 9*(11–12), 1396–1408.

Yukioka, S., Higo, Y., Noda, I., & Nagasawa, M. (1986). Correlation lengths of linear and branched polymers in a good solvent. *Polymer Journal, 18*(12), 941–946.